

TPI-MINN-97/22-T  
UMN-TH-1603/97  
hep-th/9708060

# Degeneracy and Continuous Deformations of Supersymmetric Domain Walls

M. Shifman

Theoretical Physics Institute, University of Minnesota, Minneapolis, MN 54555  
USA<sup>†</sup>

*and*

Institut für Theoretische Physik III, Universität Erlangen-Nürnberg, D-91058  
Erlangen, Germany

## Abstract

In a wide class of supersymmetric theories degenerate families of the BPS-saturated domain walls exist. The internal structure of these walls can continuously vary, without changing the wall tension. This is described by hidden parameters (collective coordinates). Differentiating with respect to the collective coordinates one gets a set of the bosonic zero modes localized on the wall. Neither of them is related to the spontaneous breaking of any symmetry. Through the residual 1/2 of supersymmetry each bosonic zero mode generates a fermionic partner.

July 1997

---

<sup>†</sup> Permanent address.

# 1 Introduction

The central extensions of  $N = 1$  superalgebras in four dimensions discovered recently [1, 2, 3, 4] lead to the existence of the BPS-saturated domain walls in supersymmetric theories, with rather peculiar properties. In Ref. [4] it was noted, in particular, that one and the same model can have a variety of distinct domain walls interpolating between the given pair of vacua. Here this remark is elaborated. It will be shown that in a wide class of supersymmetric models, typically, a (continuously degenerate) family of the domain walls exist. Each domain wall from the family is labelled by one or more hidden parameter(s). Although the internal structure of each domain wall is different, they all have one and the same energy density  $\mathcal{E}$ . One can view the domain walls from this family as bound states of two (or more) “basic” domain walls, with the vanishing binding energy. In other words, the “basic” domain walls do not interact. In the two-dimensional reductions of the four-dimensional theories under consideration the domain walls become kinks (solitons). Our result translates then into a statement that the basic “solitons” do not interact with each other.

The hidden parameters are the collective coordinates of the domain wall solutions. The existence of some collective coordinates is a trivial consequence of the fact that the domain walls spontaneously break a part of the four-dimensional symmetries: translational invariance in the  $z$  direction and 1/2 of supersymmetry (if the domain walls at hand are BPS-saturated). Therefore, the occurrence of a coordinate  $z_0$  usually referred to as the wall center, is not surprising. We will show that similar coordinates survive for each individual “component” of the “composite” BPS wall. An analogous situation takes place in the two-instanton solution of the Yang-Mills theory. Each instanton is characterized by its individual center, so that we have eight collective coordinates associated with translations, although only four translational symmetries of the theory are spontaneously broken on the solution. The symmetry of the solution is higher than that of the theory itself.

One can introduce the overall wall center,  $Z_0$ , and *extra* collective coordinates  $R_i$ , which have the physical meaning of, roughly, relative “distances” between different “components” of the wall. If all parameters  $R_i$  tend to infinity, the “basic” components of the wall are infinitely separated. The existence of such a limiting solution is trivial. The solution persists, however, at finite values of  $R_i$ , with the same tension  $\mathcal{E}$ , independent of  $R_i$ .

Differentiating with respect to the collective coordinates  $R_i$  one generates zero modes, localized on the wall and associated with a change in the internal structure of the wall. These zero modes are unrelated to the trivial zero mode corresponding to the shift of a wall, as a whole, in the  $z$  direction. Since 1/2 of supersymmetry is preserved, each extra bosonic zero mode will be accompanied by a fermionic counterpart.

The continuously degenerate domain walls occur in the models in which the parameters in the superpotential  $\mathcal{W}(\Phi, X, \dots)$  are real (or can be made real by an appropriate transformation of the fields  $\Phi, X, \dots$ ), and all extrema of the superpoten-

tial (classical minima of the potential) occur at real values of the fields  $\phi, \chi$  and so on. (Here  $\phi, \chi, \dots$  denote the lowest components of the superfields  $\Phi, X, \dots$ ). The class of theories admitting the degenerate families of the domain wall solutions is actually much wider, especially if one includes into consideration non-renormalizable and/or non-polynomial superpotentials. The latter naturally appear in effective low-energy theories, see e.g. [5, 6]. Since generalization is quite straightforward, and will become completely clear from what follows, I will limit myself here to the generalized Wess-Zumino (WZ) models [7] with renormalizable superpotentials, assuming real values of parameters, the more so that many practically important problems belong to this class.

Assume for definiteness that the superpotential  $\mathcal{W}$  has three extrema (I will call them generically  $\mathcal{M}_1, \mathcal{M}_2$  and  $\mathcal{M}_3$  where  $\mathcal{M}$  stands for a complete set of superfields in the problem at hand.) These extrema are ordered in such a way that  $\mathcal{W}(\mathcal{M}_1) < \mathcal{W}(\mathcal{M}_2) < \mathcal{W}(\mathcal{M}_3)$ . The energy density of the BPS domain walls is proportional to the central charge in the corresponding transition [1, 2], which in turn reduces to the difference of the superpotentials,

$$\varepsilon_{ij} = 2[\mathcal{W}(\mathcal{M}_j) - \mathcal{W}(\mathcal{M}_i)], \quad (1)$$

where the subscript  $ij$  marks the transition from the  $i$ -th to  $j$ -th vacuum. It is obvious then that if a family of the BPS domain walls 13 exist, all walls from this family are degenerate; their energy density is

$$\mathcal{E}(R) \equiv \varepsilon_{13} = \varepsilon_{12} + \varepsilon_{23}. \quad (2)$$

The BPS domain walls 12 and 23 are the “basic” components comprising all walls from the 13 family. As a consequence of Eq. (1) they do not interact.

The fact of existence of a family of solutions in the 13 transition can be easily established by inspecting the creek equations [4] (see also [8]) defining the BPS domain walls. There is no need in finding the actual solutions of these equations. The creek equations can be interpreted as complexified equations of motion of a high viscosity fluid (whose inertia can be neglected) on a profile associated with  $\mathcal{W}$ . For the real superpotentials and real solutions this interpretation is especially simple, since complexification becomes redundant, the profile is given just by  $-\mathcal{W}$  (with the above conventions regarding the ordering), and a very rich physical intuition everyone has in this type of motion allows one to immediately see whether or not a family of solutions exists in the given transition, by a simple examination of the profile of  $-\mathcal{W}$ .

Although the above assertions are general, I will illustrate them in the generalized WZ models describing dynamics of two chiral superfields. There is no doubt, however, that under the same circumstances degenerate families of the domain walls, with hidden parameters and a variety of zero modes corresponding to a change in the wall internal structure, appear in any model, including strongly coupled gauge

models. This may have important implications for the domain walls in supersymmetric Yang-Mills theories [3]. I will not dwell on this topic in the present paper, leaving it for future publications.

The minimal WZ model, with one chiral superfield and renormalizable superpotential, generically has only one pair of vacua, and a single BPS wall, with no hidden parameters [1, 4]. The only bosonic zero mode existing in this model is that associated with the translation of the wall as a whole. Thus, this model is uninteresting for our current purposes. To reveal the phenomenon it is necessary to consider models with two or more chiral superfields. Since all essential ingredients appear already at the level of two-field models, we will limit ourselves to two chiral superfields.

## 2 General Observations

To explain the essence of the problem it is convenient to start from a non-supersymmetric system of two real scalar fields,  $\phi$  and  $\chi$ ,

$$\mathcal{L} = \frac{1}{2} [(\partial_\mu \phi)^2 + (\partial_\mu \chi)^2 - V(\phi, \chi)] . \quad (3)$$

For a short while we will forget about the  $\phi\chi$  coupling and consider decoupled fields. We will incorporate a  $\phi\chi$  interaction term later. Assume that the self-interaction potential has a double-well shape,

$$V_0 = \left( \frac{\mu^2}{\lambda} - \lambda \phi^2 \right)^2 + \left( \frac{m^2}{g} - g \chi^2 \right)^2 , \quad (4)$$

where  $\mu$  and  $m$  are the mass terms and  $\lambda$  and  $g$  are the coupling constants. This potential has four classical minima,  $\{\phi, \chi\}_*$ ,

$$\mathcal{M}_1 = \left\{ -\frac{\mu}{\lambda}, -\frac{m}{g} \right\}, \quad \mathcal{M}_2 = \left\{ \frac{\mu}{\lambda}, -\frac{m}{g} \right\}, \quad \mathcal{M}_3 = \left\{ -\frac{\mu}{\lambda}, \frac{m}{g} \right\}, \quad \mathcal{M}_4 = \left\{ \frac{\mu}{\lambda}, \frac{m}{g} \right\} . \quad (5)$$

(It has also a maximum at the origin.) The field configuration interpolating between  $\mathcal{M}_1$  and  $\mathcal{M}_2$  is the domain wall of the  $\phi$  field,

$$\phi = \frac{\mu}{\lambda} \tanh \mu(z - z_0), \quad \chi = -\frac{m}{g}, \quad (6)$$

while that interpolating between  $\mathcal{M}_2$  and  $\mathcal{M}_4$  is the domain wall of the  $\chi$  field,

$$\phi = \frac{\mu}{\lambda}, \quad \chi = \frac{m}{g} \tanh m(z - \zeta_0), \quad (7)$$

where  $z_0$  and  $\zeta_0$  are the centers of the corresponding walls.

Finally, interpolating between the first and the fourth minima is a superposition of two previous walls,

$$\phi = \frac{\mu}{\lambda} \tanh \mu(z - z_0), \quad \chi = \frac{m}{g} \tanh m(z - \zeta_0). \quad (8)$$

The double-wall configuration (8) has two collective coordinates,  $z_0$  and  $\zeta_0$ , – not surprisingly, of course, since the fields  $\phi$  and  $\chi$  are decoupled so far, and the total energy density residing in the configuration (8) does not depend on the relation between  $z_0$  and  $\zeta_0$ , and is equal to

$$\begin{aligned} \mathcal{E}(z_0, \zeta_0) &= \varepsilon_{12} + \varepsilon_{24}, \\ \varepsilon_{12} &= \frac{4\mu^3}{3\lambda^2}, \quad \varepsilon_{24} = \frac{4m^3}{3g^2}. \end{aligned} \quad (9)$$

In other words, the two components of the domain wall configuration (8) do not interact with each other. They experience neither attraction nor repulsion. One can say that the domain wall configuration (8) is infinitely (continuously) degenerate.

The profile of the potential energy  $V_0$  is depicted on Fig. 1. The range of variation of  $\{\phi, \chi\}$  corresponding to Fig. 1 is given on Fig. 2. The wall solutions interpolating from  $A$  to  $B$  and from  $B$  to  $D$  are obviously the “basic” components of the wall solution interpolating from  $A$  to  $D$ . They are obviously unique in the sense that the  $AB$  and  $BD$  wall trajectories on Fig. 1 are unique. That’s not the case for the  $AD$  wall solution. The latter has a hidden parameter – a relative position of the components’ centers,  $R = \zeta_0 - z_0$ . If  $R = 0$  the  $AD$  wall trajectory runs right on top of the hill on Fig. 1. If  $R \neq 0$  it deviates either to the right from the top or to the left. There exists a continuous family of trajectories, with one and the same  $\mathcal{E}$ . On Fig. 2 the parameter  $R$  is reinterpreted as an angle  $\gamma$  determining the direction of motion in the initial moment of time.

(I remind that the creek interpretation of the equations defining the BPS wall [4, 8] implies that the variable  $z$  is interpreted as “time”. Correspondingly, differentiation over  $z$  will be denoted by dot, say  $\dot{\phi}$  is the  $\phi$  component of the “velocity”,  $\dot{\chi}$  is the  $\chi$  component, and so on. The angle  $\gamma$  determines the direction of the “velocity” vector,  $\gamma = \text{arccot}(\dot{\phi}/\dot{\chi})$ . For instance, for the solution (8) the angle of injection at the initial moment of time,  $z \rightarrow -\infty$ , is  $\tan \gamma = \mu^2 m^{-2} g \lambda^{-1} \exp 2(\zeta_0 - z_0)$ .)

The degeneracy is *immediately* lifted, generally speaking, once one switches on an interaction between  $\phi$  and  $\chi$ . Gone with this degeneracy is the existence of the hidden parameter and a continuous family of the  $AD$  trajectories.

Indeed, consider a typical interaction term, say,

$$\Delta V = \alpha \left( \chi^2 - \frac{m^2}{g^2} \right) \left( \phi^2 - \frac{\mu^2}{\lambda^2} \right), \quad (10)$$

to be added to  $V_0$ . The interaction is chosen in such a way that the positions of the minima of  $V$  are not shifted (Fig. 2). This is done for technical reasons only, to

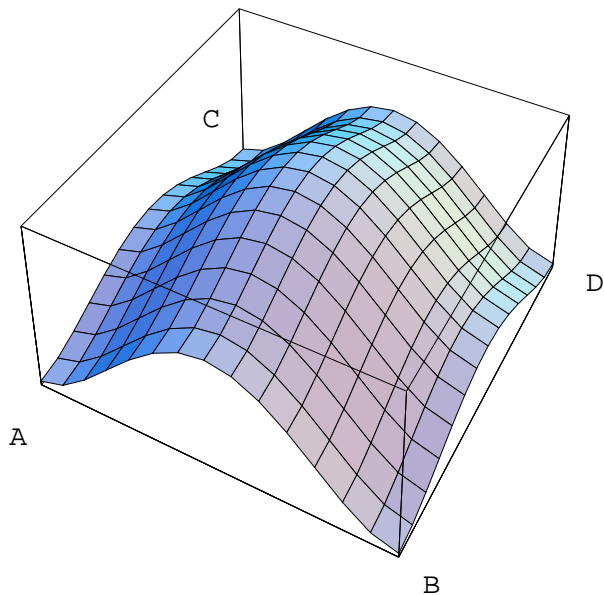


Figure 1: The potential of the two-field model given in Eq. (4) for the following values of the parameters:  $\lambda = g = 1$ ,  $\mu = 1$ ,  $m = 1.2$ . The points  $A, B, C, D$  mark four vacua of the model. The four minima  $A$  to  $D$  correspond to  $\mathcal{M}_1$  to  $\mathcal{M}_4$ , see Eq. (5).

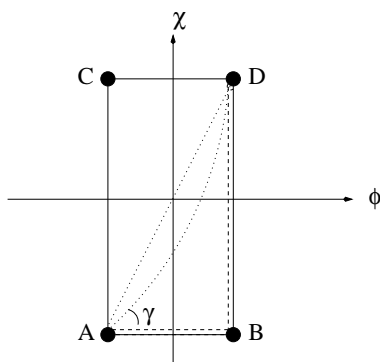


Figure 2: The range of variation of the fields  $\phi$  and  $\chi$  on the previous plot is shown by the solid line. The four minima are depicted as closed circles. The dashed lines show the wall trajectories  $AB$  and  $BD$ , while the dotted lines show two (out of infinitely many) possible  $AD$  trajectories.  $\gamma$  is the injection angle of the creek (at  $z \rightarrow -\infty$ ).

facilitate calculations. We could have easily dealt with any other interaction term. To simplify things further we will work in the limit  $\alpha \ll 1$ . This is a technical assumption too, inessential for the final conclusion.

In the first order in  $\alpha$  the change in the wall tension is

$$\Delta\mathcal{E} = \alpha \frac{\mu^2 m^2}{\lambda^2 g^2} I, \quad (11)$$

$$I = \int_{-\infty}^{\infty} dz \frac{1}{\cosh^2(\mu z)} \frac{1}{\cosh^2(m(z-R))}.$$

If  $\alpha < 0$  an attraction between the basic wall components arises; the  $AB$  and  $BD$  walls collapse, and the only wall solution connecting the points  $A$  and  $D$  that persists runs exactly on top of the hill. On the other hand if  $\alpha$  is positive, on the contrary, the basic components experience repulsion, and strictly speaking, there is no  $AD$  wall at all. It exists only as a limiting superposition of the  $AB$  and  $BD$  walls, located infinitely far from each other,  $R \rightarrow \infty$ . In the first case the angle  $\gamma$  on Fig. 2 is  $\arctan(\lambda m/g\mu)$ , in the second case it is either zero or  $\pi/2$ . In any case the collective coordinate associated with  $R$  disappears.

Even if the interaction term  $\Delta V$  is fine-tuned in such a way that classically  $\Delta\mathcal{E} = 0$ , a non-vanishing  $\Delta\mathcal{E}$  inevitably emerges at the quantum level, as a result of loop corrections, ruining the degeneracy of the  $AD$  trajectories inherent to the decoupled fields. There is no symmetry which would force  $\Delta\mathcal{E}$  to stay at zero in the non-supersymmetric case once  $\Delta V \neq 0$ , and it does not.

In contrast, it will be shown that supersymmetric BPS walls are generically continuously degenerate. In the models with two chiral superfields, besides the overall wall center, there exists one extra collective coordinate even in the presence of the  $\phi\chi$  coupling. It characterizes the wall internal structure, and is analogous to  $R$  or the angle  $\gamma$ .

Passing to the discussion of the continuous degeneracy of the domain walls in the generalized WZ models, as in the non-supersymmetric example above, it is instructive to start from two decoupled superfields. The superpotential has the form

$$\mathcal{W}_0(\Phi, X) = \left( \frac{\mu^2}{\lambda} \Phi - \frac{\lambda}{3} \Phi^3 \right) + \left( \frac{m^2}{g} X - \frac{g}{3} X^3 \right). \quad (12)$$

(I hasten to add that a  $\Phi X$  coupling will be introduced shortly.) If the lowest components of the superfields  $\Phi$  and  $X$  are denoted by  $\phi$  and  $\chi$ , the extrema of the superpotential (12) (i.e. the solutions of the equations  $\partial\mathcal{W}_0/\partial\Phi = 0$  and  $\partial\mathcal{W}_0/\partial X = 0$ ) are the same as in Eq. (5). The values of the superpotential at the extrema are

$$(\mathcal{W}_0)_* = \mp \frac{2\mu^3}{3\lambda^2} \mp \frac{2m^3}{3g^2}.$$

The profile of the function  $-\mathcal{W}_0(\Phi, X)$  is shown on Fig. 3. The first extremum,  $\mathcal{M}_1$ , is the maximum of this function,  $\mathcal{M}_4$  is the minimum,  $\mathcal{M}_{2,3}$  are the saddle points.

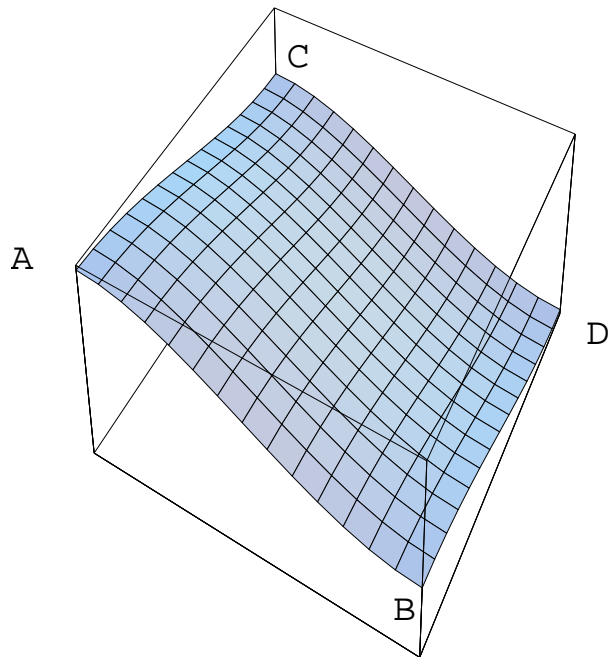


Figure 3: The profile of the superpotential  $-\mathcal{W}(\Phi, X)$ , Eqs. (12), (18). The notations are the same as on Figs. 1,2.



The  $AB$  and  $BD$  walls exist, they are given by Eqs. (6), (7). The corresponding trajectories are unique. The  $AD$  domain wall (8) represents a continuous family of trajectories, with an extra collective coordinate,  $R$  or  $\gamma$ ,

$$\gamma = \operatorname{arccot} \left( \dot{\phi} / \dot{\chi} \right)_{z \rightarrow -\infty} = \operatorname{arccot} \left[ \frac{\mu^2}{m^2} \frac{g}{\lambda} (\cosh R + \sinh R)^2 \right].$$

(Here  $R = \zeta_0 - z_0$ .) It can be viewed as a bound state of the  $AB$  and  $BD$  walls, with the vanishing binding energy.

So far, everything is in one-to-one correspondence with the situation in the decoupled non-supersymmetric example. Now comes a drastic distinction.

Let us switch an interaction term and show that:

(i) a family of the  $AD$  walls persists. This family is degenerate since for any wall from the family  $\mathcal{E} = \varepsilon_{12} + \varepsilon_{24}$ , where

$$\varepsilon_{12} = 2[\mathcal{W}(\mathcal{M}_2) - \mathcal{W}(\mathcal{M}_1)],$$

$$\varepsilon_{24} = 2[\mathcal{W}(\mathcal{M}_4) - \mathcal{W}(\mathcal{M}_2)];$$

(ii) any interaction term coupling  $\Phi$  and  $X$ , which does not cause a ‘‘catastrophic’’ restructuring of the profile  $\mathcal{W}$ , does guarantee the point (i). (I will explain later what is meant by catastrophic.)

As a matter of fact, the equality  $\mathcal{E} = \varepsilon_{12} + \varepsilon_{24}$  is a trivial consequence of the relation between the BPS wall tension and the central charge in the transition at hand, similar to Eqs. (1), (2). We need to prove only that a continuous family of the BPS trajectories, connecting the points  $A$  and  $D$  (the extrema  $\mathcal{M}_1$  and  $\mathcal{M}_4$ ) exists. In the absence of coupling between  $\Phi$  and  $X$ , the proof is explicit, see Eq. (8). When the interaction is switched on, the analytic form of the solution is unknown, but the fact of its existence follows from the creek equations [4, 8]

$$\vec{\dot{\Phi}} = \vec{\nabla} \overline{\mathcal{W}}. \tag{13}$$

(Here  $\vec{\Phi}$  is a generic set of the superfields; under the rules of the game we have accepted, one can drop the bar over  $\mathcal{W}$  on the right-hand side.) We will prove two straightforward consequences of Eq. (13).

I). An infinite number of the wall trajectories originate from every maximum of  $(-\mathcal{W})$ , and infinitely many trajectories end up in every minimum.

II). Only one trajectory departs from every saddle point of  $(-\mathcal{W})$ , and only one arrives.

Needless to say that, since we are speaking of maxima, minima and saddle points, we continue dealing, as previously, only with the real solutions of the creek equations (13), assuming all parameters in the superpotential to be real. In the complex plane all extrema are saddle points, of course.

To prove the assertions (I) and (II) above consider the profile  $\mathcal{W}(\Phi, X)$  near the extremum points. Near the extrema

$$\mathcal{W} = \mathcal{W}_* + P_2(\delta\Phi, \delta X)$$

where

$$\delta\Phi = \Phi - \Phi_*, \quad \delta X = X - X_*,$$

and  $P_2$  is a homogeneous polynomial of the second order. By a real rotation of the fields  $\delta\Phi, \delta X$ ,

$$\{\delta\Phi, \delta X\} \rightarrow \{\Delta_1, \Delta_2\}$$

one can always diagonalize  $P_2$ . In terms of the diagonal variables  $\Delta_{1,2}$

$$P_2 = \frac{1}{2}A\Delta_1^2 + \frac{1}{2}B\Delta_2^2,$$

where  $A, B$  are some constants, and the creek equations take the form

$$\dot{\Delta}_1 = A\Delta_1, \quad \dot{\Delta}_2 = B\Delta_2. \quad (14)$$

Both constants,  $A$  and  $B$  are positive near the maximum of  $-\mathcal{W}$ , negative near the minimum, and one positive one negative near the saddle points. The appropriate asymptotic behavior of the trajectory is  $\Delta_{1,2} \rightarrow 0$  at  $z \rightarrow -\infty$  for the outgoing trajectory, and at  $z \rightarrow \infty$  for the incoming trajectory. The solutions of Eqs. (14) with the appropriate asymptotics are

$$\Delta_1 = C_1 e^{Az}, \quad \Delta_2 = C_2 e^{Bz} \quad (15)$$

for the trajectories leaving a maximum or arriving at a minimum of  $-\mathcal{W}$ . Here  $C_{1,2}$  are arbitrary constants, whose ratio determines  $\gamma$ . At the same time for the trajectories attached to the saddle points we have

$$\Delta_1 = C_1 e^{Az}, \quad \Delta_2 = 0 \quad (16)$$

and

$$\Delta_1 = 0, \quad \Delta_2 = C_2 e^{Bz}. \quad (17)$$

The first one leaves a saddle point, the second arrives (I assume for definiteness that  $A > 0, B < 0$ .) It is quite obvious that in Eq. (15) a continuous parameter emerges, while there is no such freedom in the case of Eqs. (16), (17).

Not every trajectory leaving a maximum will end up at a minimum (or at a saddle point, a special case), thus generating a legitimate BPS wall. Some trajectories will lead to abysses, yielding no BPS-saturated domain wall solutions. In other words, there are global constraints on the angle  $\gamma$ . These constraints become clear from a visual examination of the profile of  $-\mathcal{W}$ . Thus, in the trivial case of Eq. (12) the boundary values of the angle are  $\gamma_* = 0$  and  $\gamma_* = \pi/2$ . Introducing an interaction

between  $\Phi$  and  $X$  we shift the vacuum values of the fields  $\Phi_*, X_*$ , the corresponding values of the superpotential (determining the central charges), the boundary values  $\gamma_*$ , but as long as the interaction term does not cause a “geographical” disaster, the continuous degeneracy of the  $AD$  wall family will survive, the model will support a unique trajectory for the  $AB$  and  $BD$  walls, and a continuous family for the  $AD$  walls.

A typical interaction is

$$\Delta\mathcal{W} = 2\alpha\Phi X, \quad \mathcal{W} = \mathcal{W}_0 + \Delta\mathcal{W}. \quad (18)$$

The coupling between  $\Phi$  and  $X$  distorts details of the profile, as compared with the decoupling limit, but the gross features remain the same: one maximum, one minimum, two saddle points. The maximum of  $-\mathcal{W}$  is the highest point, the saddle points are somewhat below, and the minimum of  $-\mathcal{W}$  is the lowest point. Starting from the maximum, the creek descends to either of the saddle points, from either of the saddle points it descends to the minimum. Finally, there is a family of trajectories connecting the maximum and the minimum directly. What particular trajectory is chosen, depends on the angle  $\gamma$  of the stream injection at the initial moment of time (i.e.  $z \rightarrow -\infty$ ). If  $\alpha \ll |\mu - m|$  the boundary value of  $\gamma$ , instead of zero, becomes  $\gamma_* = \alpha|\mu - m|^{-1} + O(\alpha^2)$ .

Other couplings between  $\Phi$  and  $X$ , not necessarily reducing to Eq. (18), are possible too. The general pattern will continue to hold until the interaction between  $\Phi$  and  $X$  becomes so strong that the gross features of the “slope” under consideration change – e.g. a new “mountain ridge” emerges preventing the descent to the minimum, or the minimum raises up to the level of the maximum, and so on. This can only happen under special conditions, at  $\alpha \sim |\mu - m|$ . This catastrophic restructuring is a different story, however, which will not be touched in the present paper. As long as the coupling between  $\Phi$  and  $X$  does not change the overall general pattern of the extrema on the “slope”, a continuous family of the  $AD$  walls will exist.

### 3 Elaborating a Specific Example.

To get further insight on the impact the continuously degenerate BPS wall families may have, it is instructive to work out particular models. Therefore, I choose a concrete coupling between  $\Phi$  and  $X$ , and rewrite the two-field model at hand in a slightly different form by passing to new superfields (which I will still continue calling  $\Phi$  and  $X$ ),

$$\mathcal{W} = \frac{m^2}{\lambda}\Phi - \frac{\lambda}{3}\Phi^3 - \alpha\Phi X^2. \quad (19)$$

The four extrema  $\{\Phi, X\}_*$  are

$$\mathcal{M}_1 = \left\{-\frac{m}{\lambda}, 0\right\}, \quad \mathcal{M}_{2,3} = \left\{0, \pm\frac{m}{\sqrt{\lambda\alpha}}\right\}, \quad \mathcal{M}_4 = \left\{\frac{m}{\lambda}, 0\right\}. \quad (20)$$

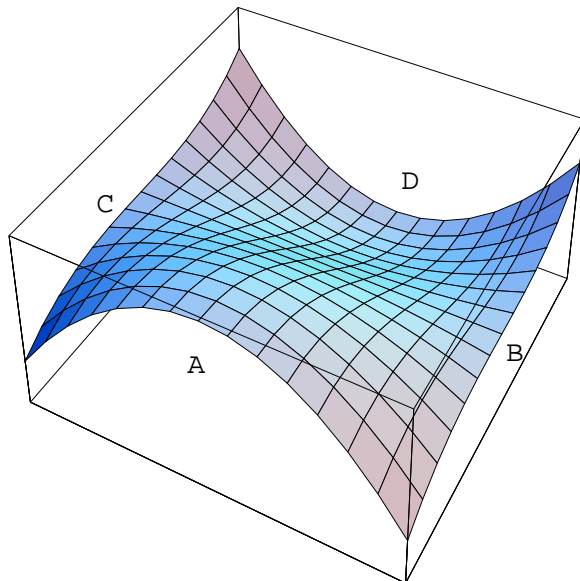


Figure 4: The profile of the superpotential  $-\mathcal{W}$  in the model (19) for the following values of the parameters:  $\lambda = m = 1$ ,  $\alpha = 0.49$ . The points  $A, B, C, D$  mark four vacua of the model:  $A$  is maximum of  $-\mathcal{W}$  corresponding to  $\mathcal{M}_1$ ,  $D$  is minimum corresponding to  $\mathcal{M}_4$ ,  $B, C$  are saddle points  $\mathcal{M}_{2,3}$ .

The values of the superpotential at extrema are

$$\mathcal{W}(\mathcal{M}_1) = -\frac{2}{3} \frac{m^3}{\lambda^2}, \quad \mathcal{W}(\mathcal{M}_{2,3}) = 0, \quad \mathcal{W}(\mathcal{M}_4) = \frac{2}{3} \frac{m^3}{\lambda^2}. \quad (21)$$

The profile of the corresponding function  $-\mathcal{W}$  is shown on Fig. 4, while the scalar potential in the model at hand is presented on Fig. 5. The essential points are explained on Fig. 6. It is assumed that  $\alpha < \lambda$ . As we will see shortly, the relation between  $\alpha$  and  $\lambda$  is important.

At  $\alpha \neq \lambda$  the only apparent symmetry of the model (19) (additionally to supersymmetry) is a discrete  $Z_4$ ,

$$\Phi \rightarrow \pm\Phi \quad \text{and} \quad X \rightarrow \pm X. \quad (22)$$

This symmetry connects the vacua  $\mathcal{M}_1$  and  $\mathcal{M}_4$ , or  $\mathcal{M}_2$  and  $\mathcal{M}_3$ :  $\mathcal{M}_1$  is physically equivalent to  $\mathcal{M}_4$  while  $\mathcal{M}_2$  equivalent to  $\mathcal{M}_3$ .  $Z_4$  is spontaneously broken down to  $Z_2$  in any of the four vacuum states. No symmetry relates  $\mathcal{M}_1$  to  $\mathcal{M}_2$ .

As previously,  $A$  marks the maximum,  $D$  the minimum, and  $B, C$  mark the saddle points. The walls  $AB$  and  $AC$  are equivalent, and so are the walls  $BD$  and  $CD$ . The domain walls  $AD$  and  $BC$  are different. The first one is BPS, while the second is non-BPS; their tensions do not coincide.

The ellipse depicted on Fig. 6 by a thick solid line, as well as the horizontal axis, also depicted by a thick solid line, are level lines – they give the zero of the

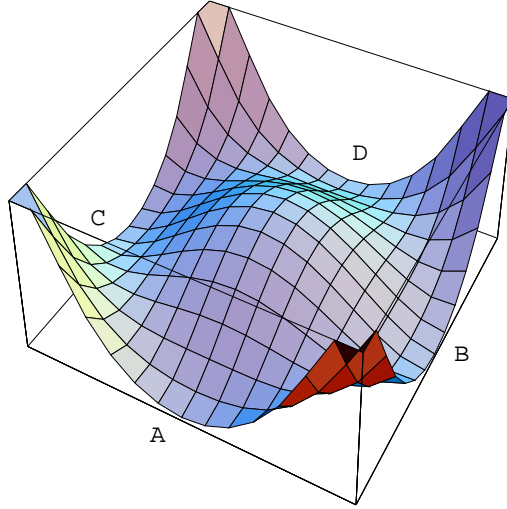


Figure 5: The scalar potential in the same model.

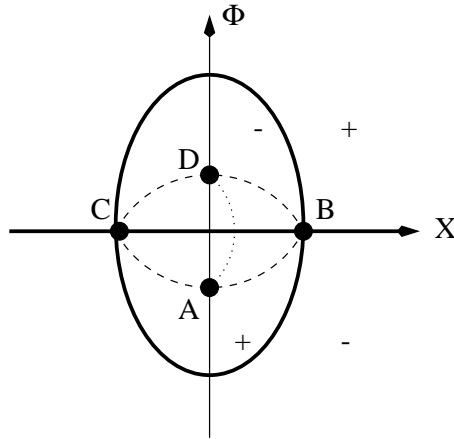


Figure 6: The map of  $\Phi$  and  $X$ , for the previous plots, with the level lines. The thick solid lines denote zero of the superpotential  $-\mathcal{W}$ , Eq. (19). The regions of the positive height are marked by pluses, the regions of the negative height by minuses. The dashed lines denote the trajectories of the BPS walls coming to (or leaving from) the saddle points. The dotted line is one of (infinitely many) possible  $AD$  walls.

superpotential. Pluses and minuses indicate the height of  $-\mathcal{W}$  in the corresponding regions (positive or negative). The dashed line  $BACD$  is the boundary of the region where a continuous family of the degenerate  $AD$  trajectories lies. Any trajectory leaving the point  $A$  with the “velocity” directed in the lower half-plane will end up in abyss, while those with the “velocity” in the upper half-plane will arrive at the point  $D$ . One of such trajectories is depicted by the dotted line. The corresponding wall tension is

$$\mathcal{E} = \frac{8 m^3}{3 \lambda^2}. \quad (23)$$

Two trajectories are exceptional; they lead from  $A$  to  $C$  or  $B$ . The energy density of these walls is

$$\varepsilon = \frac{4 m^3}{3 \lambda^2}. \quad (24)$$

The dashed line  $BAC$  is the edge of the mountain ridge, while the dashed line  $CDB$  is the bottom of a valley. By inspecting the matrix of the second derivatives of  $\mathcal{W}$  one readily convinces oneself that the dashed line is horizontal at the points  $A$  and  $D$ , while it approaches the saddle points  $B$  and  $C$  at the angles  $\pm\pi/4$ . It is pretty obvious that the creek leaving  $B$  at  $-\pi/4$  will arrive at  $D$ . If  $\alpha < \lambda/2$ , the boundary trajectories from the  $AD$  family can be found analytically,

$$\Phi = \frac{m}{\lambda} \tanh(Mz), \quad X = \pm \frac{m}{\sqrt{\alpha\lambda}} \sqrt{1 - \frac{2\alpha}{\lambda}} \frac{1}{\cosh(Mz)}, \quad (25)$$

where

$$M = \frac{2\alpha m}{\lambda}.$$

For these trajectories at  $z \rightarrow -\infty$  the “velocities” are horizontal.

Instead of analyzing the creek equations, one could prove the existence of the continuously degenerate family of the  $AD$  walls in an indirect way, by counting the fermion zero modes using the index theorem [9]. A symmetric solution of the creek equation,

$$X = 0, \quad \Phi = \frac{m}{\lambda} \tanh(mz) \quad (26)$$

obviously exists. Now, if one calculates the matrix of the second derivatives (the fermion mass matrix)  $\partial^2 \mathcal{W} / \partial \Phi_i \partial \Phi_j$  on the solution (26), this matrix is diagonal,

$$\partial^2 \mathcal{W} / \partial \Phi_i \partial \Phi_j = -2 \text{diag}\{\lambda \Phi, \alpha \Phi\},$$

with *both* eigenvalues changing sign along the trajectory (26). From the index theorem [9] we then learn of the existence of two fermion zero modes. Since the solution (26) preserves 1/2 of supersymmetry, each fermion zero mode must have a boson partner. Thus, we must have two boson zero modes. One is associated with a shift of the wall center, another reflects the possibility of shifting the trajectory along the “slope” (i.e. changing the internal structure of the wall) without changing the tension.

### 3.1 Non-BPS wall connecting the saddle points $\mathcal{M}_2$ and $\mathcal{M}_3$

Since the points  $B$  and  $C$  both lie at zero of the superpotential, there is no BPS wall connecting them [1, 4]. A non-BPS wall exists. The corresponding value of  $\Phi = 0$ , while  $X(z)$  satisfies the second-order equation

$$\frac{d^2 X}{dz^2} = -2\alpha X \left( \frac{m^2}{\lambda} - \alpha X^2 \right). \quad (27)$$

Its solution is

$$X = \frac{m}{\sqrt{\lambda\alpha}} \tanh(Mz), \quad M = \sqrt{\frac{\alpha}{\lambda}} m. \quad (28)$$

A straightforward calculation of the tension of the  $BC$  wall yields

$$\tilde{\mathcal{E}} = \sqrt{\frac{\lambda}{\alpha}} \frac{8}{3} \frac{m^3}{\lambda^2} = \sqrt{\frac{\lambda}{\alpha}} 2\varepsilon. \quad (29)$$

At  $\alpha < \lambda$  the energy density of the non-BPS wall (28) is higher than the sum of the energy densities of the BPS walls connecting  $BD$  and  $DC$ , see Eq. (24). The wall (28) is classically unstable with respect to the decay into two BPS walls  $BD$  and  $DC$ , separated by an infinite  $\Delta z$  interval. How the instability begins to develop is clearly seen from Fig. 5. If we start from the solution (28), with  $\Phi = 0$ , it is energetically expedient to push the trajectory away from the top of the hill in the  $\Phi$  direction. Quantitatively, one can analyse the Hamiltonian for  $\Phi$  in the background (28), assuming that  $\Phi(z)$  is small, i.e. keeping only the quadratic terms in  $\Phi$  and omitting higher orders. The mode equation for  $\Phi$  takes the form

$$\left\{ -\frac{d^2}{dz^2} + M^2 \left[ 4 - \left( 4 + \frac{2\lambda}{\alpha} \right) \frac{1}{\cosh^2(Mz)} \right] \right\} \Phi_n(z) = E_n \Phi_n(z) \quad (30)$$

with the boundary conditions

$$\Phi_n(z \rightarrow \pm\infty) = 0.$$

The parameter  $M$  is the same as in Eq. (28).

At  $\alpha < \lambda$  the lowest mode  $\Phi_0$  is negative,  $E_0 < 0$ . This means that allowing the wall trajectory to slide down in the direction of  $\Phi_0$ ,

$$\Phi \sim \Phi_0,$$

we make the energy density of the  $BC$  wall lower than that in Eq. (29). This is the way the instability in Eq. (28) starts. The evolution of the instability ends when the wall (28) breaks into two well-separated pieces, two BPS walls connecting  $\mathcal{M}_2$  to  $\mathcal{M}_4$  and  $\mathcal{M}_4$  to  $\mathcal{M}_3$ , respectively.

If  $\alpha > \lambda$ , on the contrary, the above two BPS walls are attracted to each other. They form a stable bound state, a non-BPS wall (28), connecting  $\mathcal{M}_2$  to  $\mathcal{M}_3$  directly. The wall tension  $\tilde{\mathcal{E}}$  is smaller than the sum of the tensions of the  $BD$  and  $DC$  walls.

Note, that the tensions of the BPS walls are calculated exactly, while those of the non-BPS walls, generally speaking, receive corrections due to quantum loops. If the coupling constants are small, these corrections are small too, and can be neglected everywhere except in the immediate vicinity of the point  $\alpha = \lambda$ .

The point  $\alpha = \lambda$  is special. At this point the tension of the non-BPS wall  $BC$  is exactly equal to the sum of the tensions of the  $BD$  and  $DC$  walls and equal to the tension of the BPS wall  $AD$ ,

$$\tilde{\mathcal{E}} = 2\varepsilon = \mathcal{E}. \quad (31)$$

This is due to the fact that at  $\alpha = \lambda$  the model (19) degenerates into a system of two decoupled superfields  $(\Phi \pm X)/\sqrt{2}$ , and the  $BC$  wall becomes physically identical to the  $AD$  one. Thus, although an additional symmetry emerges at  $\alpha = \lambda$ , this limit is uninteresting.

### 3.2 Integrating out a heavy field

In many applications one has to deal with effective Lagrangians which are written for light degrees of freedom after one integrates out heavy degrees of freedom. An example which is widely discussed now is the effective Lagrangian for the supersymmetric Yang-Mills theory [5, 6]. Here we show that, integrating out heavy fields, typically one erases any trace of the continuous degeneracy of the BPS walls existing before the heavy degrees of freedom are eliminated.

Let us turn again to the model (19), and consider the limit  $\alpha \gg \lambda$ . Then in the vacua  $\mathcal{M}_1$  and  $\mathcal{M}_4$  the field  $X$  is much heavier than  $\Phi$ ,

$$\frac{M_X}{M_\Phi} = \frac{\alpha}{\lambda}. \quad (32)$$

As a matter of fact, this ratio holds (almost) everywhere along the trajectory connecting  $\mathcal{M}_1$  and  $\mathcal{M}_4$ . The only exception is at  $\Phi = 0$ . Therefore, following a standard routine, one is tempted to integrate out the field  $X$  in order to obtain an effective Lagrangian for the “light” field  $\Phi$ . The standard routine is based on the Born-Oppenheimer procedure: one freezes the value of  $\Phi$ , and for every given value finds an optimal value of  $X$  minimizing the energy of the field configuration at hand. In this way one finds that for all values of  $\Phi$  (except  $\Phi = 0$ , but we will forget about this one “singular” point, as it is commonly done) the corresponding optimal value of  $X$  vanishes, as a consequence of the equation  $\partial\mathcal{W}/\partial X = 0$ . Substituting this solution back to  $\mathcal{W}(\Phi, X)$  given in Eq. (19), we arrive at the effective Lagrangian for the  $\Phi$  field, representing nothing but the minimal WZ model. As is well-known [1, 4], the wall solution in this model is unique. Thus, integrating out  $X$  à la Born-Oppenheimer we lose any possibility of exploring the continuous family of the BPS walls, which exists in the full theory. It is highly probable that a similar situation may take place in the Veneziano-Yankielowicz effective Lagrangian [5] (see also [3]), where an uncontrollable number of “heavy” degrees of freedom is eliminated. Whether this is the case, and if so, what is the dimension of the parameter



space of the BPS walls in the supersymmetric Yang-Mills theories remains an open question.

## **Acknowledgments**

I would like to thank M. Voloshin for a discussion. This work was done during my stay at Institut für Theoretische Physik III, Universität Erlangen-Nürnberg. I am grateful to F. Lenz and other members of the group for kind hospitality.

This work was supported in part by DOE under the grant number DE-FG02-94ER40823 and by Alexander von Humboldt-Stiftung.

## References

- [1] G. Dvali and M. Shifman, hep-th/9611213 [Nucl. Phys. B, to appear].
- [2] G. Dvali and M. Shifman, *Phys. Lett.* **B396** (1997) 64.
- [3] A. Kovner, M. Shifman and A. Smilga, hep-th/9706089 [Phys. Rev. D, submitted].
- [4] B. Chibisov and M. Shifman, hep-th/9706141 [Phys. Rev. D, submitted].
- [5] G. Veneziano and S. Yankielowicz, *Phys. Lett.* **B113** (1982) 231.
- [6] A. Kovner and M. Shifman, hep-th/9702174 [Phys. Rev. D, to appear].
- [7] J. Wess and B. Zumino, *Phys. Lett.* **B49** (1974) 52.
- [8] E.R.C. Abraham and P.K. Townsend, *Nucl. Phys.* **B351** (1991) 313;  
M. Cvetič, F. Quevedo and S.-J. Rey, *Phys. Rev. Lett.* **67** (1991) 1836.
- [9] R. Jackiw and C. Rebbi, *Phys. Rev.* **D13** (1976) 3398;  
E. Weinberg, *Phys. Rev.* **D24** (1981) 2669.